Solvation potentials for flexible chain molecules in solution: On the validity of a pairwise decomposition

Mark P. Taylor[a] and Gregory M. Petersen
Department of Physics, Hiram College, Hiram, Ohio 44234, USA

(Received 20 June 2007; accepted 28 August 2007; published online 9 November 2007)

The effects of a solvent on the conformation of a flexible n-site solute molecule can be described formally in terms of an n-body solvation potential. Given the practical difficulty in computing such multibody potentials, it is common to carry out a pairwise decomposition in which the n-body potential is approximated by a sum of two-body potentials. Here we investigate the validity of this two-site approximation for short interaction-site chain-in-solvent systems. Using exact expressions for the conformation of an isolated chain, we construct a mapping between the full chain-in-solvent system and its solvation potential representation. We present results for both hard-sphere and square-well systems with $n=5$ that show that the two-site approximation is sufficient to completely capture the effects of an explicit solvent on chain conformation for a wide range of conditions (which include varying the solvent diameter in the hard-sphere system and varying the chain-solvent coupling in the square-well system). In all cases, a *set* of two-site potentials (one for each distinct site-site pair) is required. We also show that these two-site solvation potentials can be used to accurately compute a multisite intramolecular correlation function. © *2007 American Institute of Physics*. [DOI: 10.1063/1.2787006]

I. INTRODUCTION

The conformation of a flexible chain molecule in solution is intrinsically coupled to the properties of the solvent. For dilute polymer solutions it is usual to broadly classify solvents as being "good," "poor," or "theta" for a particular polymer.[1–3] In a good solvent a polymer chain is in an expanded or open conformation, maximizing solvent polymer contact. Conversely, in a poor solvent a polymer chain is in a compact or collapsed conformation, minimizing exposure to the solvent. The theta solvent corresponds to a special intermediate condition in which the long-range intrachain excluded volume interactions (which tend to expand the chain) are effectively "screened out" by the solvent. Under such theta conditions many properties of the polymer resemble those of an ideal or Gaussian chain. In most cases the "quality" of a solvent also depends on external variables such as temperature and pH and thus solvent quality can be tuned via adjustment of these parameters.

In much of the theoretical work on polymers in dilute solution, the effects of solvent have been treated in an implicit fashion.[2–9] Thus it is common to consider an isolated chain with a repulsive potential as a model for a polymer in good solvent. Similarly, an isolated self-avoiding chain with an intrachain attractive potential can be used both to model a polymer in poor solvent and, with appropriate adjustment of the potential strength, to also model a chain in a theta solvent. This implicit treatment of solvent is based on the assumption that the multibody effects of a solvent interacting with a chain molecule can be represented through a pairwise effective potential acting between the sites of the polymer chain.[4] The purpose of the present work is to investigate the validity of this commonly used pairwise solvation potential approximation.

We study this problem of explicit solvent effects on chain conformation using an interaction-site model for the chain-in-solvent system. Here we model solvent as a simple liquid comprised of spherically symmetric interaction sites (e.g., hard, square-well, or Lennard-Jones spheres) while a chain molecule is modeled as a set of such interaction sites bonded together by "universal joints" (i.e., a pearl-necklace-type model). Such a completely flexible interaction-site chain provides a coarse-grained model of a chain molecule in which each interaction site is meant to represent several chemical repeat units of a real chain.[10] These simple interaction-site chain-in-solvent systems display interesting solvent effects.[11–25] For example, a hard-sphere chain is found to be compressed by the addition of a hard-sphere solvent with the degree of compression increasing monotonically with solvent density and being a function of the relative solvent/chain-site size ratio.[11–14] A purely entropic chain collapse transition has been reported for a hard-sphere chain in a dense hard-sphere solvent with solvent/chain-site size ratio of 5. In the case of a square-well (SW) or Lennard-Jones (LJ) chain-in-solvent system, both solvent induced chain compression and chain expansion are possible.[15–19] In particular, at low temperatures the SW (LJ) solvent tends to expand the SW (LJ) chain while at high temperatures chain compression is observed. The role of explicit solvent in the chain collapse transition for these thermal systems has also been investigated.[20–23]

It is in fact possible to construct an exact implicit treatment of the above described explicit solvent effects in a chain-in-solvent system. Such an exact mapping from an

[a]Electronic mail: taylormp@hiram.edu

n-site chain molecule in solvent to a single-chain system is formally provided by an n-body solvation potential.[26] This n-body potential, which is constructed by integrating out the solvent degrees of freedom, depends on the exact conformation of the chain and is, in general, not practical to compute. Thus one typically resorts to an approximate pairwise decomposition of this multibody potential.[26–37] Although the validity of this decomposition has been questioned,[27,38] to our knowledge, no direct tests have been reported for a chain in explicit solvent. It seems clear that this approximation must break down for a long chain in the poor solvent limit (where different chain sites will have very different solvent exposures);[20] however, the question of whether the approximation is actually valid under any circumstances remains open. Here we analyze this question for interaction-site-model chain-in-solvent systems over a range of solvent conditions. Our approach involves exact calculations for the conformation of a single chain[39–41] and is thereby limited to short ($n \leqslant 5$) chains. Some preliminary results for a hard-sphere system are reported in Ref. 42.

II. THE INTERACTION-SITE CHAIN-IN-SOLVENT MODEL

A. Intramolecular probability functions

Here we consider a linear chain molecule comprised of n spherically symmetric interaction sites attached by completely flexible universal joints of fixed bond length L. The chain is immersed in a monomeric solvent consisting of N solvent particles contained in a volume V (solvent density $\rho=N/V$) at temperature T. The chain sites are located by the set of position vectors $\{\mathbf{r}_i\}$ and the interaction energy between two nonbonded chain sites is given by $u_{ij}=u(r_{ij})$, with $i<j+1$, where $i,j \in \{1,\ldots,n\}$ and $r_{ij}=|\mathbf{r}_i-\mathbf{r}_j|$. Similarly, the solvent molecules are located by the set of position vectors $\{\mathbf{R}_k\}$ and the interaction energy between two solvent molecules is given by $\nu_{kl}=\nu(R_{kl})$, with $k \neq l$, where $k,l \in \{1,\ldots,N\}$ and $R_{kl}=|\mathbf{R}_k-\mathbf{R}_l|$. Finally, the interaction energy between a chain site and a solvent molecule is given by $w_{ik}=w(|\mathbf{r}_i-\mathbf{R}_k|)$. For a fixed chain and solvent configuration, the total chain-chain, solvent-solvent, and chain-solvent interaction energies are given, respectively, as follows:

$$U_n(\{\mathbf{r}_i\}) = \sum_{i<j+1}^{n} u_{ij}, \tag{1a}$$

$$V_N(\{\mathbf{R}_k\}) = \sum_{k<l}^{N} \nu_{kl}, \tag{1b}$$

$$W_{n+N}(\{\mathbf{r}_i\},\{\mathbf{R}_k\}) = \sum_{i,k}^{n,N} w_{ik}. \tag{1c}$$

The probability density that the n-site chain will be found in a specific conformation $\{\mathbf{r}_i\}$ (i.e., that each chain site i will be located within an infinitesimal volume element $d\mathbf{r}_i$ about position $\mathbf{r}_i$) is given by[14,43]

$$P_n(\{\mathbf{r}_i\};\rho,T) = \frac{e^{-\beta U_n} S_n}{Z_{n+N}(\rho,T)} \int \cdots \int e^{-\beta V_N} e^{-\beta W_{n+N}} d\{\mathbf{R}_k\}, \tag{2}$$

where $\beta=1/k_BT$, k_B is the Boltzmann constant, $Z_{n+N}(\rho,T)$ is the canonical partition function defined to give the normalization

$$\frac{1}{V} \int \cdots \int P_n(\{\mathbf{r}_i\};\rho,T) d\{\mathbf{r}_i\} = 1, \tag{3}$$

and

$$S_n = \prod_{i=1}^{n-1} s_{i,i+1} \tag{4}$$

is the product of the intramolecular distribution functions $s_{ab}=\delta(r_{ab}-L)/4\pi L^2$ between bonded sites.

While the n-site intramolecular probability function given in Eq. (2) provides a complete specification of the chain conformation, it is generally too cumbersome to work with directly. Thus one resorts to reduced versions of this function and here we will primarily work with the set of two-site probability functions given by

$$P_{ij}(r_{ij};\rho,T) = 4\pi r_{ij}^2 \int \cdots \int P_n(\{\mathbf{r}_i\};\rho,T) \prod_{m\neq i,j}^{n} d\mathbf{r}_m. \tag{5}$$

These two-site probability functions allow for the calculation of mean-square site-site distances

$$\langle r_{ij}^2 \rangle = \int_0^{|i-j|L} r_{ij}^2 P_{ij}(r_{ij};\rho,T) dr_{ij} \tag{6}$$

and thus, the mean-square radius of gyration

$$\langle R_g^2 \rangle = \frac{1}{n^2} \sum_{i<j}^{n} \langle r_{ij}^2 \rangle, \tag{7}$$

which is an experimentally accessible measure of average chain size.

B. The solvation potential mapping

The intramolecular probability functions for a chain in solvent, given by Eqs. (2) and (5), are formidable objects to compute since they both contain a $3N$-dimensional integral over all solvent configurations. One can formally simplify these expressions by introducing an n-site solvation potential $U_n^{\mathrm{sol}}(\{\mathbf{r}_i\};\rho,T)$ which completely accounts for the effects of the solvent on chain conformation.[26] In this approach one maps from the chain-in-solvent system to an isolated chain interacting via an effective potential given by

$$U_n^{\mathrm{eff}}(\{\mathbf{r}_i\};\rho,T) = U_n(\{\mathbf{r}_i\}) + U_n^{\mathrm{sol}}(\{\mathbf{r}_i\};\rho,T). \tag{8}$$

Thus the n-site probability function for the chain in solvent takes on the form of a single-chain probability function as follows:[39–41]

$$P_n(\{\mathbf{r}_i\};\rho,T) = \frac{e^{-\beta U_n^{\text{eff}}(\rho,T)} S_n}{Z_n(\rho,T)}, \tag{9}$$

where

$$Z_n(\rho,T) = \frac{1}{V}\int \cdots \int e^{-\beta U_n^{\text{eff}}(\rho,T)} S_n d\{\mathbf{r}_i\}. \tag{10}$$

In practice Eq. (9) is no more tractable than Eq. (2) due to the difficulty in actually computing the n-body solvation potential. However, one can greatly simplify the chain-in-solvent problem by assuming a pairwise decomposition of this n-body potential.[26–29] In this approximation, one writes the n-body solvation potential as a sum of two-site solvation potentials

$$U_n^{\text{sol}}(\{\mathbf{r}_i\};\rho,T) = \sum_{i<j+1}^{n} u_{ij}^{\text{sol}}(r_{ij};\rho,T), \tag{11}$$

and thus the chain-in-solvent problem becomes that of an isolated chain with effective site-site interactions given by

$$u_{ij}^{\text{eff}}(r_{ij};\rho,T) = u_{ij}(r_{ij}) + u_{ij}^{\text{sol}}(r_{ij};\rho,T). \tag{12}$$

The site-site probability functions for this effective-potential chain can be written as[40]

$$P_{ij}(r;\rho,T) = \frac{4\pi r^2 e^{-\beta u_{ij}^{\text{eff}}(r;\rho,T)}}{Z_n(\rho,T)} D_{ij}^{(n)}(r;\rho,T), \tag{13}$$

where the $D_{ij}^{(n)}(r;\rho,T)$ functions are $3(n-2)$-dimensional integrals given by

$$D_{ij}^{(n)}(r;\rho,T) = \int \cdots \int S_n \prod_{\substack{a<b+1 \\ a,b\neq i,j}}^{n} e^{-\beta u_{ab}^{\text{eff}}(r_{ab};\rho,T)} \prod_{m\neq i,j}^{n} d\mathbf{r}_m \tag{14}$$

and the single-chain partition function can be written in terms of any one of the set of $D_{ij}^{(n)}$ functions as follows:

$$Z_n(\rho,T) = 4\pi \int_0^{|i-j|L} r^2 e^{-\beta u_{ij}^{\text{eff}}(r;\rho,T)} D_{ij}^{(n)}(r;\rho,T) dr. \tag{15}$$

Equation (13) is the basis for the numerous studies of polymer chains in solution in which the solvent is treated implicitly. This commonly used approach, in which the site-site potentials for a single chain are assumed to include a solvent contribution [as in Eq. (12)], is clearly premised on the two-site approximation of Eq. (11). Furthermore, in such implicit solvent studies, one usually assumes that a single site-site potential acts between nonbonded beads on the chain and thus that a single site-site solvation potential is sufficient to account for solvent effects.

In this work we examine the validity of this type of implicit solvent treatment. More fundamentally, we will investigate whether or not the two-site decomposition of the multibody solvation potential given by Eq. (11) is appropriate for any chain-in-solvent system. To carry out this test, we rewrite Eq. (13) as follows:

$$\beta u_{ij}^{\text{eff}}(r;\rho,T) = \ln\left(4\pi r^2 \frac{D_{ij}^{(n)}(r;\rho,T)}{P_{ij}(r;\rho,T)}\right) - \ln(Z_n(\rho,T)), \tag{16}$$

where the term involving the single-chain partition function is to be treated as an additive constant which sets the zero of the energy. Given a set of site-site probability functions $P_{ij}(r;\rho,T)$ for a chain in solvent (which can be obtained, for example, from a first principles density expansion or from a full chain-in-solvent Monte Carlo simulation),[14] Eq. (16) can be viewed as a set of coupled integral equations for the corresponding set of site-site effective potentials (and thus site-site solvation potentials) $\{u_{ij}^{\text{eff}}\}$, with $i<j+1$, where $i,j \in \{1,\ldots,n\}$. In order to test the two-site approximation, one simply attempts to find a self-consistent solution to this set of coupled equations. The question of whether or not this set of equations actually has a solution is the crux of our investigation. An affirmative answer to this question will provide strong (numerical) evidence in support of the validity of the two-site approximation. Furthermore, assuming that a solution to Eq. (16) *is* possible, comparison of the resulting set of site-site effective potentials will show whether or not a single effective potential is sufficient to completely account for solvent effects. [We note that each of these effective potentials is only defined up to an additive constant and thus the set of coupled equations represented by Eq. (16) is in fact formally unchanged by replacing the set $\{u_{ij}^{\text{eff}}\}$ with the set $\{u_{ij}^{\text{eff}}+C_{ij}\}$ where each C_{ij} may be a different constant.]

Before proceeding with our numerical analysis, we would like to point out that the two-site solvation potential approximation is in fact rigorously valid for the 3-mer chain-in-solvent system. In this case $D_{13}^{(3)}(r)=1/(8\pi L^2 r)$ (see Ref. 40) and the site-site effective potential is given exactly by

$$\beta u_{13}^{\text{eff}}(r;\rho,T) = -\ln\left(\frac{L^2}{2r} P_{13}(r;\rho,T)\right) - \ln(Z_3(\rho,T)),$$

$$0 \leqslant r \leqslant 2L, \tag{17}$$

where, as noted above, the term involving the single-chain partition function can be treated as an additive constant which sets the zero of the energy.

C. Site-site potentials and numerical methods

The developments of the above sections are applicable to any chain-in-solvent system with spherically symmetric site-site potentials. In this work we restrict our attention to hard-sphere and square-well systems. For the hard-sphere system, the chain and solvent hard-sphere diameters are denoted by σ and D, respectively, and the chain bond length is set to $L=\sigma$. The interaction potentials for this system are $u_{ij}(r)=u^{\text{HS}}(r;\sigma,\sigma)$, $\nu_{kl}(r)=u^{\text{HS}}(r;D,D)$, and $w_{ik}(r)=u^{\text{HS}}(r;\sigma,D)$ where the hard-sphere potential is given by

$$u^{\text{HS}}(r;d_a,d_b) = \begin{cases} \infty, & r < (d_a+d_b)/2 \\ 0, & r > (d_a+d_b)/2 \end{cases}. \tag{18}$$

For the square-well system, we keep the chain and solvent sites the same size so that the chain-chain and solvent-solvent interaction energies are both given by $u_{ij}(r)=\nu_{kl}(r)=u^{\text{SW}}(r;\lambda)$ where the square-well potential is

$$u^{\mathrm{SW}}(r;\lambda)=\begin{cases}\infty, & r<\sigma\\ -\varepsilon, & \sigma<r<\lambda\sigma\\ 0, & r>\lambda\sigma\end{cases}. \tag{19}$$

We allow for a variable chain-solvent interaction[23] given by $w_{ik}(r)=\alpha u^{\mathrm{SW}}(r;\lambda)$ where α is a chain-solvent coupling parameter $(0\leqslant\alpha\leqslant 1)$ defined such that $\lim_{\alpha\to 0}[\alpha u^{\mathrm{SW}}(r;\lambda)]=u^{\mathrm{HS}}(r;\sigma,\sigma)$. The chain bond length is set to $L=\sigma$ and the square-well depth ε sets the temperature scale via the reduced temperature $T^*=k_BT/\varepsilon$. In the limit of $T^*\to\infty$ this square-well system becomes identical to the $D=\sigma$ hard-sphere system.

Our attempt to map the above chain-in-solvent systems to an isolated chain representation requires a self-consistent solution to Eq. (16). This mapping will only be feasible for short chains due to the difficulty in computing the multidimensional D_{ij} integrals [Eq. (14)]. Here we carry out calculations for chains up to length $n=5$ using the explicit expressions for the D_{ij} integrals given in Ref. 40. Gauss-Legendre quadrature is used to evaluate these integrals with special care being taken at site-site distances where the $P_{ij}(r)$ functions exhibit discontinuous behavior $(\sigma+L,\ \lambda\sigma,$ and $\sigma+\lambda\sigma)$.[39] The set of coupled equations given by Eq. (16) is solved on a grid using a Picard iteration scheme[44] with the input $P_{ij}(r)$ values being established on the grid via quadratic interpolation/extrapolation[45] (taking care at the distances noted above). Our criterion for convergence is that the input and output sets of $\{u_{ij}^{\mathrm{eff}}\}$ functions differ by no more that 10^{-6} at each position grid point. Since Eq. (16) only defines the effective potentials up to an arbitrary additive constant, we fix one point of each potential to be zero throughout the calculation. (In fact, we set the potentials to zero beyond this cutoff point which is taken as $r=2.0\sigma$ for $|i-j|=2$, $r=2.9\sigma$ for $|i-j|=3$, and $r\leqslant 3.6\sigma$ for $|i-j|=4$).

The site-site probability functions $P_{ij}(r)$, which appear in Eq. (16), are obtained from chain-in-solvent Monte Carlo (MC) simulations. Details of the hard-sphere simulations are given in Ref. 14 and the square-well simulations are discussed in Ref. 19. We use both single-site axial rotation[46] and multisite pivotlike translation moves for the chain.[47] For the simulation data presented here, we use between 100 and 3000 solvent particles in a rectangular box with periodic boundary conditions and between 10^7 and 4×10^9 Monte Carlo cycles. We report results in terms of the solvent volume fraction η which is slightly smaller than the total particle volume fraction in the simulation box $(\eta_{\mathrm{total}}=\eta+n\pi\sigma^3/6V)$. For the results presented here, we use enough solvent particles such that the fractional difference between these two values is less than or equal to 2% [i.e., $(\eta_{\mathrm{total}}-\eta)/\eta\leqslant 0.02$]. In all cases the minimum dimension of the simulation box exceeds the stretched length of the chain plus several solvent diameters. Block averaging is used to estimate uncertainties and the equilibration time (which equals the block length) is chosen such that the chain end-to-end distance covers the range of values from near contact to near full chain extension.

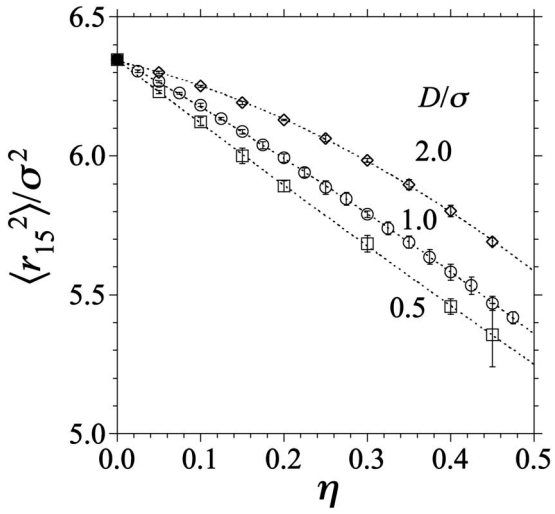

FIG. 1. Mean-square end-to-end distance $\langle r_{15}^2\rangle$ vs solvent volume fraction η for a hard-sphere 5-mer chain with site diameter σ in a hard-sphere solvent with solvent diameters $D=2\sigma$, $D=\sigma$, and $D=0.5\sigma$ as indicated. The filled symbol for $\eta=0$ is an exact result (see the Appendix) while the open symbols for $\eta>0$ are results from full chain-in-solvent MC simulations. The lines are meant as a guide for the eyes only.

III. RESULTS

A. Hard-sphere systems

The primary effect of a hard-sphere solvent on a hard-sphere chain is chain compression (i.e., a reduction in the average chain size relative to the isolated chain).[12–14] This behavior is seen in Fig. 1 where we show Monte Carlo results for the average size of a hard-sphere 5-mer chain in hard-sphere solvent with solvent diameters $D=2\sigma$, σ, and $\sigma/2$ for solvent volume fractions $\eta=\pi D^3/6$ up to $\eta=0.475$ (the hard-sphere freezing transition occurs at $\eta\approx 0.49$).[44] The compression effect is seen to increase with both increasing solvent volume fraction and decreasing solvent diameter.

In Fig. 2 we show site-site probability functions for this 5-mer hard-sphere chain-in-solvent system for solvent volume fractions $\eta=0.45$ for $D=\sigma$ and 2σ and $\eta=0.40$ for $D=\sigma/2$. The end-to-end probability function for an isolated hard-sphere chain (i.e., $\eta=0$) is included to illustrate the strong solvent perturbation to the local chain structure. The central question of this study is as follows: Can these strong solvent induced perturbations to local chain structure be reproduced using an effective potential in a single-chain calculation? To answer this question we attempt to find a self-consistent solution to the set of four coupled equations (for u_{15}^{eff}, u_{14}^{eff}, u_{13}^{eff}, and u_{24}^{eff}) represented by Eq. (16) using Monte Carlo data, such as that shown in Fig. 2, for the required P_{ij} functions. We are in fact able to solve these equations and the resulting sets of solvation potentials, obtained from the Monte Carlo data of Fig. 2, are shown in Fig. 3. All of these potentials display a deep attractive well for small site-site separations as expected for a potential that produces chain compression. To verify that our calculations are self-consistent, we use Eq. (13) to compute the site-site probability functions for an isolated 5-mer chain interacting via the effective potentials shown in Fig. 3. The results of these single-chain calculations are included as the solid lines

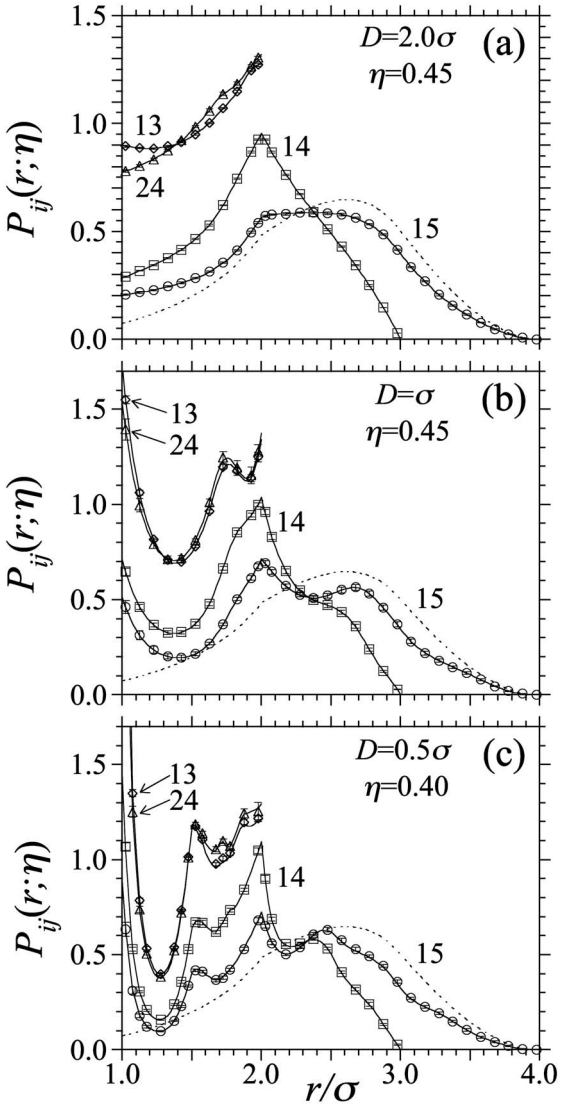

FIG. 2. Site-site probability functions $P_{ij}(r,\eta)$ for sites i and j as indicated vs site-site distance r for a hard-sphere 5-mer chain with site diameter σ in a hard-sphere solvent at volume fraction $\eta=0.45$ with solvent diameters (a) $D=2\sigma$, (b) $D=\sigma$, and (c) at $\eta=0.40$ with $D=0.5\sigma$. The symbols are results from full chain-in-solvent MC simulations while the lines are results of exact single-chain calculations using Eq. (13) and the two-site solvation potentials shown in Fig. 3. In each case, the dashed line shows the end-to-end probability function for an isolated (i.e., $\eta=0$) 5-mer chain. Some MC data points have been omitted for clarity. In part (c) the off-scale contact values are $P_{13}(\sigma)\approx 3.7$ and $P_{24}(\sigma)\approx 3.3$.

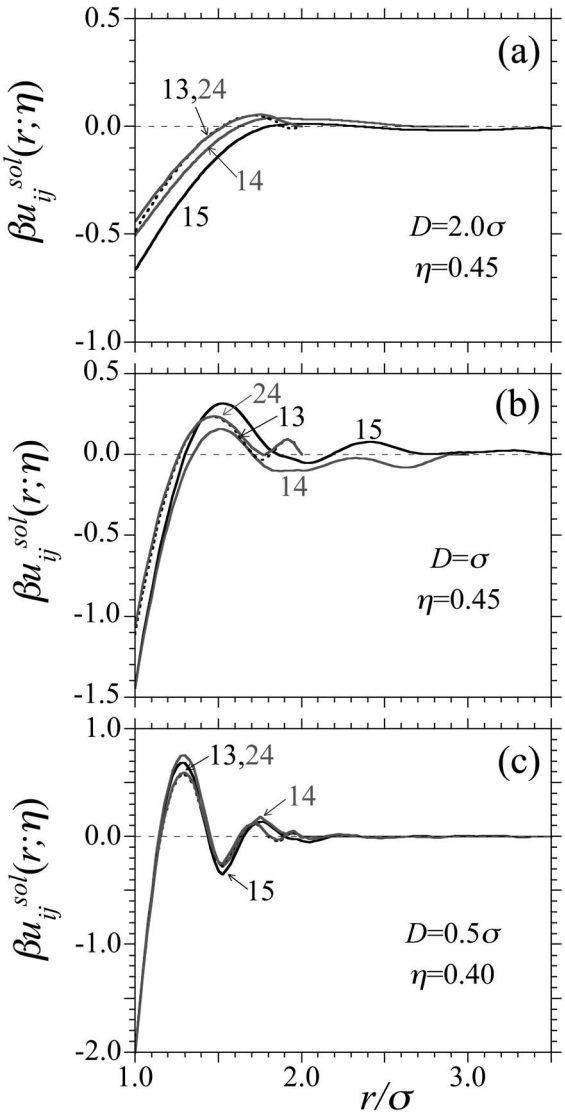

FIG. 3. Two-site solvation potentials $u_{ij}^{\mathrm{sol}}(r,\eta)$ for sites i and j as indicated vs site-site distance r for a hard-sphere 5-mer chain with site diameter σ in a hard-sphere solvent at volume fraction $\eta=0.45$ with solvent diameters (a) $D=2\sigma$, (b) $D=\sigma$, and (c) at $\eta=0.40$ with $D=0.5\sigma$. These potentials were obtained through a self-consistent solution of the set of coupled integral equations represented by Eq. (16) using the MC data shown in Fig. 2.

shown in Fig. 2. As seen in this figure, the single-chain calculations "exactly" match the results of the full chain-in-solvent simulation. We have carried out this calculation for each of the state points shown in Fig. 1 with identical success in each case. We have also carried out this calculation for chains of lengths $n=3$ and 4 and find equally good results (some of which are shown in Ref. 42). For the cases with $n>3$ we require a set of solvation potentials and thus the question of the uniqueness of these sets of functions arises. Although we have no mathematical proof of uniqueness for our calculated sets of solvation potentials, we have found in all cases considered that our numerical procedure converges to an apparently unique set of potentials (i.e., our numerical solutions appear to be independent of the initial guess used to start the iteration).

B. Square-well systems

To further assess the general validity of the pairwise decomposition of the multibody solvation potential, we have carried out the same type of analysis described in the previous section for square-well chain-in-solvent systems. In a system with attractive interactions, solvent effects can include chain expansion in addition to chain compression. This behavior is seen in Fig. 4 where we show Monte Carlo results for the average size of a 5-mer square-well chain in a square-well solvent with $\lambda=1.5$ and $\alpha=1.0$ (the critical point for this solvent is given by $T_c^*=1.22$ and $\eta_c=0.162$).[48] The chain is compressed with increasing solvent density at high temperatures while it is expanded by the solvent (at least at low solvent density) at low temperatures. For the $\lambda=1.5$, $\alpha=1.0$, 5-mer chain system, the crossover temperature between regimes of expansion and compression is $T^*\approx 5.0$.[17,19] Another effect of the square-well solvent (with $\alpha=1$) on the

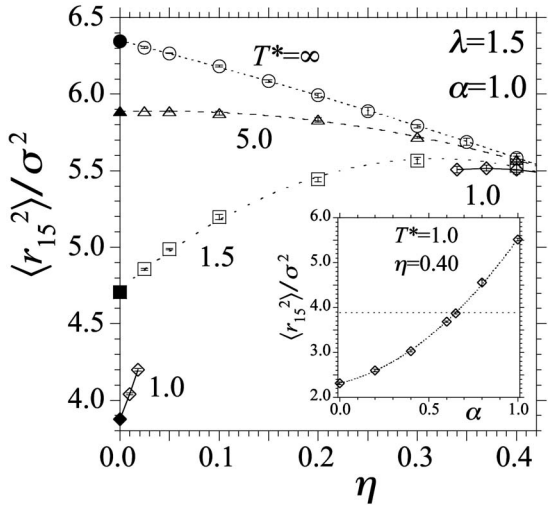

FIG. 4. Mean-square end-to-end distance $\langle r_{15}^2 \rangle$ vs solvent volume fraction η for a square-well 5-mer chain in a square-well solvent with $\lambda=1.50$ and $\alpha=1.0$ at reduced temperatures $T^*=\infty$, 5.0, 1.5, and 1.0 as indicated. The filled symbols for $\eta=0$ are exact results (see the Appendix) while the open symbols for $\eta>0$ are results from full chain-in-solvent MC simulations. The critical temperature for this solvent is $T^*\approx 1.22$ and thus the results for $T^*=1.0$ are interrupted by a two-phase region spanning the range $0.018 \leqslant \eta \leqslant 0.34$ (Ref. 48). The inset shows the chain size vs solvent-chain coupling parameter α for the case of $T^*=1.0$, $\eta=0.40$. In all cases, the lines are meant as a guide for the eyes only.

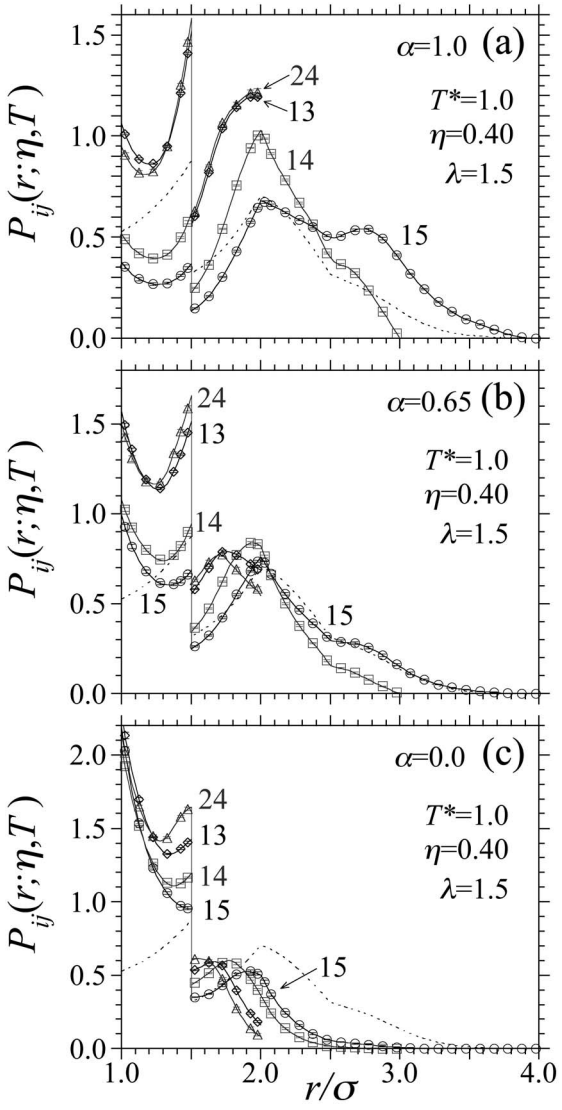

FIG. 5. Site-site probability functions $P_{ij}(r;\eta,T^*)$ for sites i and j as indicated vs site-site distance r for a square-well ($\lambda=1.5$) 5-mer chain in a square-well ($\lambda=1.5$) solvent at volume fraction $\eta=0.40$, temperature $T^*=1.0$, and with chain-solvent coupling parameter (a) $\alpha=1$, (b) $\alpha=0.65$, and (c) $\alpha=0$. The symbols are results from full chain-in-solvent MC simulations while the lines are results of exact single-chain calculations using Eq. (13) and the two-site solvation potentials shown in Fig. 6. In each case the dashed line shows the end-to-end probability function for an isolated (i.e., $\eta=0$) 5-mer chain at $T^*=1.0$.

square-well chain is the inhibition of chain collapse at high solvent density. This is seen in Fig. 4 for $\eta=0.40$ where the chain remains expanded as the temperature is reduced from $T^*=\infty \rightarrow T^*=1.0$ [for this same temperature reduction, the isolated chain ($\eta=0$) begins to collapse]. Both chain expansion and this inhibition of chain collapse are due to "solvation" of the chain by the solvent. By reducing the chain-solvent coupling parameter α, the stabilizing effects of the solvent are reduced and the chain undergoes a collapse transition that is enhanced by the presence of the solvent.[22,23] This is shown in the inset to Fig. 4 where we see that for $T^*=1.0$, $\eta=0.40$, as the chain-solvent coupling is reduced from $\alpha=1 \rightarrow \alpha=0$, the chain collapses to a size significantly smaller than that of the isolated ($\eta=0$) chain at this temperature.

As an illustration of our test of the two-site solvation potential approximation for SW systems, we consider a SW chain in a subcritical (liquid phase) SW solvent with $\eta=0.40$ and $T^*=1.0$ for a range of chain-solvent coupling parameters α (see Fig. 4 inset). In particular, we examine the two extreme situations of solvent induced chain expansion (i.e., good solvent behavior) seen for $\alpha=1$ and solvent enhanced chain collapse (i.e., poor solvent behavior) seen for $\alpha=0$. We also consider the special intermediate case of $\alpha=0.65$ where the average chain size is unchanged by the presence of solvent (thetalike conditions). Monte Carlo results for the site-site probability functions for these three cases are shown in Fig. 5. As for the hard-sphere systems, these MC data are used in Eq. (16), which is solved self-consistently to obtain the solvation potentials shown in Fig. 6. The set of solvation potentials for $\alpha=1$ displays a large repulsive barrier which leads to chain expansion while the $\alpha=0$ potentials display a broad attractive well resulting in chain compression. For the intermediate case of $\alpha=0.65$, both an attractive well and repulsive barrier are present resulting in no net change in average chain size. When these solvation potentials are used in the single-chain calculation given by Eq. (13), the resulting single-chain site-site probability functions, shown as the lines in Fig. 5, exactly match the full chain-in-solvent Monte Carlo results, thus verifying the validity of the two-site approximation (for short chains) across the full range of solvent conditions.

C. Multibody correlations

Thus far our test of the validity of the pair decomposition of the multibody solvation potential has involved calculating solvent effects at the level of two-site probability functions. A more rigorous test of the pair decomposition would

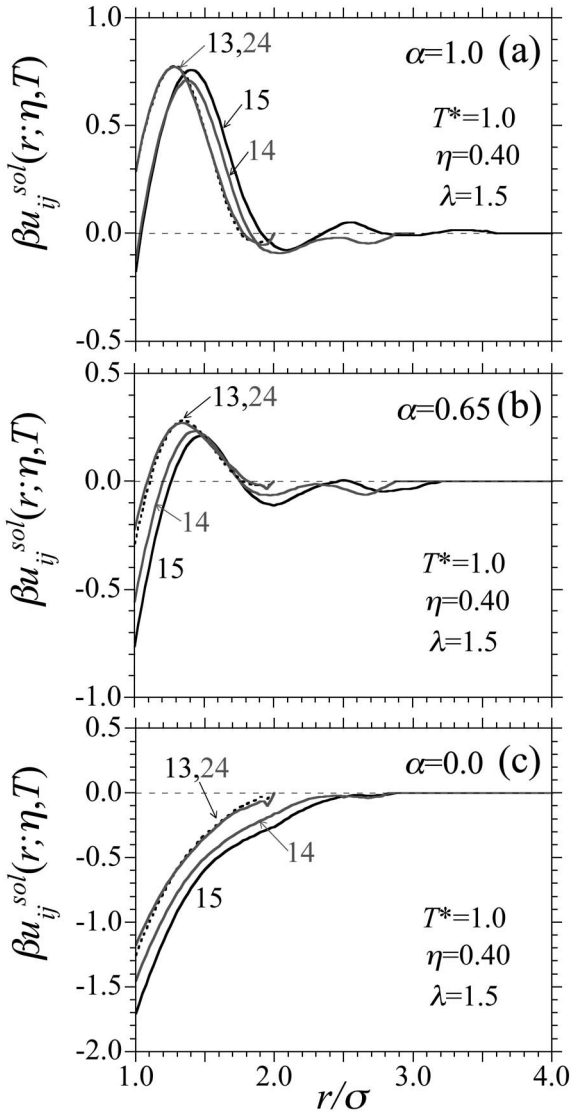

FIG. 6. Two-site solvation potentials $u_{ij}^{\mathrm{sol}}(r;\eta,T^*)$ for sites i and j as indicated vs site-site distance r for a square-well ($\lambda=1.5$) 5-mer chain in a square-well ($\lambda=1.5$) solvent at volume fraction $\eta=0.40$, temperature $T^*=1.0$, and with chain-solvent coupling parameter (a) $\alpha=1$, (b) $\alpha=0.65$, and (c) $\alpha=0$. These potentials were obtained through a self-consistent solution of the set of coupled integral equations represented by Eq. (16) using the MC data shown in Fig. 5.

be to compute higher order correlation functions starting from the two-site solvation potentials. An example of such a higher order correlation function for a 4-mer chain molecule is the four-body site-site probability function $P_4(r_{13},r_{24})$. This particular function has been studied by Grayce for the hard-sphere chain-in-solvent system.[38] For an isolated 4-mer chain, this function can be written exactly as[39,40]

$$P_4(r_{13},r_{24}) = \frac{1}{Z_4}\frac{r_{13}r_{24}}{4\pi L^4}e^{-\beta(u_{13}+u_{24})}\int_0^{\pi} e^{-\beta u_{14}}d\varphi, \tag{20}$$

where the required 1–4 site-site distance is given by

$$r_{14}^2 = L^2 + \frac{r_{13}r_{24}}{2L^2}\{r_{13}r_{24} - [(4L^2 - r_{13}^2)(4L^2 - r_{24}^2)]^{1/2}\cos\varphi\} \tag{21}$$

and we have the reduction property

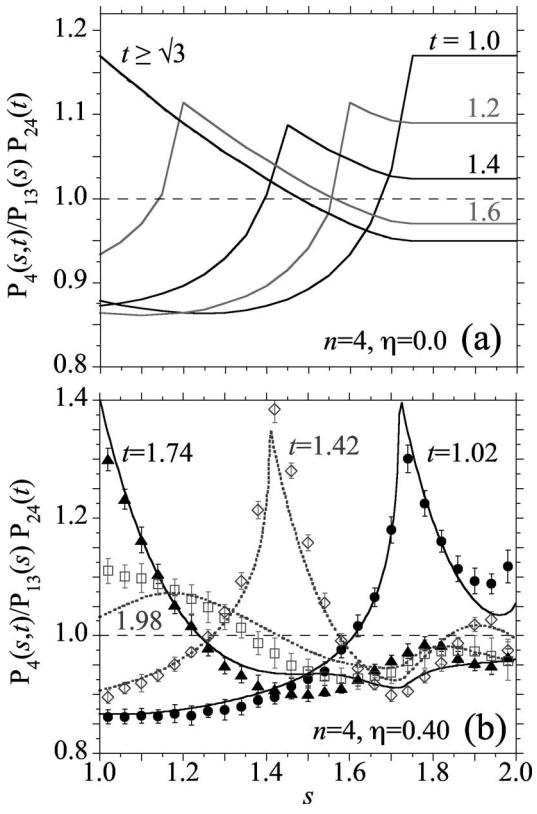

FIG. 7. Multisite correlation function $P_4(s,t)/P_{13}(s)P_{24}(t)$ for values of $t=r_{24}/\sigma$ as indicated vs site-site distance $s=r_{13}/\sigma$ for a hard-sphere 4-mer chain. In (a) we show exact results for an isolated chain and in (b) we show results for the chain in hard-sphere solvent with $D=\sigma$ and $\eta=0.40$. The symbols in (b) are results from a full chain-in-solvent MC simulation while the lines are results of a single-chain calculation [Eq. (20)] with a set of two-site solvation potentials constructed as described in the text.

$$P_{13}(r) = P_{24}(r) = \int_0^{2L} P_4(r,s)ds. \tag{22}$$

In Fig. 7(a) we show this multibody function [divided by the uncorrelated value $P_{13}(r_{13})P_{24}(r_{24})$] for the isolated ($\eta=0$) hard-sphere chain with $L=\sigma$. As seen in this plot, the r_{13} and r_{24} site-site distances are correlated such that an overall chain configuration with one of these distances large and the other small is more probable than predicted by the product of the individual two-site probabilities. This correlation displays a maximum when $r_{13}^2+r_{24}^2=4L^2$ (for r_{13} or $r_{24}<\sqrt{3}$) which corresponds to a crossover to conformations in which the minimum r_{14} distance exceeds σ.

In Fig. 7(b) we show this multibody function for the hard-sphere 4-mer in hard-sphere solvent with $D=\sigma$ at volume fraction $\eta=0.40$. Results are shown both from a full chain-in-solvent simulation and from the single-chain calculation given by Eq. (20) using a set of effective (solvation) potentials $\{u_{14}^{\mathrm{eff}},u_{13}^{\mathrm{eff}}\}$ determined as described above (and shown in Ref. 42). The solvent is seen to have a strong effect on this correlation function with the peaks observed for the isolated chain both growing in magnitude and narrowing with increasing solvent density. (These peaks correspond to the ridge of positive correlation seen in Grayce's contour plot representation of this function shown in Ref. 38.) Although the agreement between the two-site solvation potential ap-

TABLE I. Equation (A1) expansion coefficients for square-well 5-mer chains with well diameter $\lambda=1.5$. The mean-square end-to-end distance for the hard-sphere ($T^*=\infty$) 5-mer chain is $\langle r_{15}^2\rangle/\sigma^2=6.3458$.

	k						
	0	1	2	3	4	5	6
$c_k(1.5)$	0.748 75	0.926 46	0.473 23	0.169 80	0.039 86	7.878×10^{-3}	3.496×10^{-4}
$g_k(1.5)$	0.082 06	0.135 31	0.090 57	0.046 26	0.014 47	4.012×10^{-3}	2.222×10^{-4}

proximation and the Monte Carlo data for this multibody correlation function is not as exact as for the two-site probability functions, it is quite good (improving with reduced solvent density) and certainly captures the detailed structure of the chain in solvent.

IV. DISCUSSION

In this work we have carried out a direct test of the validity of a pair decomposition of the multibody solvation potential for a flexible chain in a monomeric solvent. We find that this two-site solvation potential approximation is nearly exact for hard-sphere and square-well chain-in-solvent systems for chains up to length $n=5$. We have carried out this test up to very high solvent volume fractions ($\eta\leqslant0.475$ for the hard-sphere system and $\eta\leqslant0.425$ for the $\lambda=1.5$ square-well system) and for a range of solvent conditions resulting in both expanded and nearly collapsed square-well chains. We have also examined the case of a critical solvent (i.e., $\eta=0.162$, $T^*=1.22$ for the $\lambda=1.5$ square-well fluid)[48] and find equally good solvation potential results. Testing this approximation for longer chains is difficult due to the required computation of a set of multidimensional integrals [Eq. (14)] similar to the integrals encountered when evaluating higher order virial coefficients. Although we certainly expect the two-site approximation to break down under certain conditions for longer chains (especially in the case of a collapsed chain with solvent inaccessible "interior" sites),[20] we have at least established that there are cases for which the approximation can be considered correct.

One important result is the finding that a set of site-site potentials is required for this mapping between the chain-in-solvent system and the effective-potential chain representation. Thus, the implicit inclusion of solvent via a single site-site effective potential (which is a common approach) cannot, in general, be expected to completely capture solvent induced perturbations to chain conformation. An exception to this may be the case of a small solvent/chain-site size ratio. As seen in Fig. 3(c), for the hard-sphere chain-in-solvent system with $D=0.5\sigma$, the four site-site solvation potentials are nearly identical. We note that these potentials have the structure of a "depletion" potential for two large spheres in a fluid of small spheres, including the expected repulsive barrier and secondary minimum.[49]

We have also reported the interesting finding that for short hard-sphere chains, this two-site approximation allows for the accurate calculation of multibody correlation functions. This to some extent resolves the open question as to whether or not a full multibody solvation potential is essential in capturing such structural details.[38] At this point we have only examined the single multibody correlation function reported above; however, we plan to extend our investigation in an attempt to further clarify this question.

Finally, we have recently proposed a method that makes use of the exact short-chain solvation potentials computed here to construct solvation potentials for long chain molecules.[42] This construction is motivated by the observation that the local structure of short and long interaction-site chains is often quite similar. Thus we make the assumption that our short chain effective potentials can be applied to "nearby" sites along the backbone of a long chain. We make the further assumption that for a solvent with $D=\sigma$, the solvation potential approaches the solvent potential of mean force for sites distant along the chain backbone. Our approach interpolates between these limits to build a complete set of effective potentials for a long chain. Our initial results for this construction for hard-sphere systems are quite promising and we are continuing to investigate this approach. Further results will be reported in a forthcoming publication.

ACKNOWLEDGMENTS

M.P.T. thanks Jutta Luettmer-Strathmann for numerous helpful discussions and Brad Goodner for providing use of the Hiram College Center for Deciphering Life's Language computer cluster (funded by HHMI Undergraduate Science Education Grant No. 52005125). Financial support was provided by the Hiram College and the Donors of the American Chemical Society Petroleum Research Fund.

APPENDIX: SIZE OF AN ISOLATED SQUARE-WELL 5-MER CHAIN

The size of an isolated 5-mer square-well chain can be computed exactly following the density of states calculation presented in Ref. 41. In particular, the mean-square end-to-end distance for a 5-mer chain with well-diameter λ at reduced temperature T^* can be expressed exactly as

$$\langle r_{15}^2(\lambda,T^*)\rangle=\sigma^2\sum_{k=0}^{6}c_k(\lambda)e^{k/T^*}\Bigg/\sum_{k=0}^{6}g_k(\lambda)e^{k/T^*}. \tag{A1}$$

Results for the expansion coefficients $c_k(\lambda)$ and $g_k(\lambda)$ for $\lambda=1.5$ are given in Table I.

[1] P. J. Flory, *Principles of Polymer Chemistry* (Cornell University Press, Ithaca, 1953).
[2] J. des Cloiseaux and G. Jannink, *Polymers in Solution* (Clarendon, Oxford, 1990).
[3] A. Yu. Grosberg and A. R. Khokhlov, *Statistical Physics of Macromolecules* (AIP, New York, 1994).
[4] W. H. Stockmayer, Macromol. Chem. Phys. **35**, 54 (1960).
[5] F. L. McCrackin, J. Mazur, and C. M. Guttman, Macromolecules **6**, 859

(1973).
[6] A. Baumgartner, J. Chem. Phys. **72**, 871 (1980).
[7] A. Milchev, W. Paul, and K. Binder, J. Chem. Phys. **99**, 4786 (1993).
[8] J. M. Wichert and C. K. Hall, Macromolecules **27**, 2744 (1994); J. Duatenhahn and C. K. Hall, *ibid.* **27**, 5399 (1994).
[9] M. Wittkop, S. Kreitmeier, and D. Goritz, J. Chem. Phys. **104**, 3373 (1996); Macromolecules **29**, 4754 (1996).
[10] K. Binder, in *Monte Carlo and Molecular Dynamics Simulations in Polymer Science*, edited by K. Binder (Oxford University Press, New York, 1995), Chap. 1.
[11] J. Komorowski and W. Bruns, J. Chem. Phys. **103**, 5756 (1995).
[12] F. A. Escobedo and J. J. de Pablo, Mol. Phys. **89**, 1733 (1996).
[13] J. K. C. Suen, F. A. Escobedo, and J. J. de Pablo, J. Chem. Phys. **106**, 1288 (1997).
[14] M. P. Taylor, J. Chem. Phys. **121**, 10757 (2004).
[15] G. Luna-Barcenas, D. G. Gromov, J. C. Meredith, I. C. Sanchez, J. J. de Pablo, and K. P. Johnston, Chem. Phys. Lett. **278**, 302 (1997).
[16] G. Luna-Barcenas, J. C. Meredith, I. C. Sanchez, K. P. Johnston, D. G. Gromov, and J. J. de Pablo, J. Chem. Phys. **107**, 10782 (1997).
[17] M. Lisal and I. Nezbeda, J. Chem. Phys. **119**, 4026 (2003); Fluid Phase Equilib. **222**, 247 (2004).
[18] J. A. Porter and J. E. G. Lipson, J. Chem. Phys. **122**, 094906 (2005).
[19] M. P. Taylor, J. Chem. Phys. **123**, 167101 (2005).
[20] R. Chang and A. Yethiraj, J. Chem. Phys. **114**, 7688 (2001).
[21] J. M. Polson and M. J. Zuckermann, J. Chem. Phys. **116**, 7244 (2002).
[22] J. M. Polson and N. E. Moore, J. Chem. Phys. **122**, 024905 (2005).
[23] S. B. Opps, J. M. Polson, and N. A. Risk, J. Chem. Phys. **125**, 194904 (2006).
[24] H. H. Gan and B. C. Eu, J. Chem. Phys. **109**, 2011 (1998).
[25] S. Mendez, J. G. Curro, M. Puetz, D. Bedrov, and G. D. Smith, J. Chem. Phys. **115**, 5669 (2001).
[26] D. Chandler and L. R. Pratt, J. Chem. Phys. **65**, 2925 (1976).
[27] P. E. Smith and B. M. Pettitt, J. Phys. Chem. **98**, 9700 (1994).
[28] C. N. Likos, Phys. Rep. **348**, 267 (2001).
[29] C. J. Grayce and K. S. Schweizer, J. Chem. Phys. **100**, 6846 (1994).
[30] C. J. Grayce, A. Yethiraj, and K. S. Schweizer, J. Chem. Phys. **100**, 6857 (1994).
[31] C. J. Grayce and J. J. de Pablo, J. Chem. Phys. **101**, 6013 (1994).
[32] M. P. Taylor and J. E. G. Lipson, Fluid Phase Equilib. **150**, 641 (1998).
[33] K. F. Freed, J. Chem. Phys. **116**, 10475 (2002).
[34] Y. Ye, J. D. McCoy, and J. G. Curro, J. Chem. Phys. **119**, 555 (2003).
[35] T. Sumi and H. Sekino, J. Chem. Phys. **122**, 194910 (2005).
[36] L. Livadaru and A. Kovalenko, J. Phys. Chem. B **109**, 10631 (2005).
[37] J. R. Silbermann, S. H. L. Klapp, M. Schoen, N. Chennamsetty, H. Bock, and K. E. Gubbins, J. Chem. Phys. **124**, 074105 (2006).
[38] C. J. Grayce, J. Chem. Phys. **106**, 5171 (1997).
[39] M. P. Taylor, Mol. Phys. **86**, 73 (1995).
[40] M. P. Taylor, J. Chem. Phys. **114**, 6472 (2001).
[41] M. P. Taylor, J. Chem. Phys. **118**, 883 (2003).
[42] M. P. Taylor and S. Ichida, J. Polym. Sci., Part B: Polym. Phys. **45**, 3319 (2007).
[43] T. L. Hill, *Statistical Mechanics* (Dover, New York, 1956).
[44] J. P. Hanson and I. R. McDonald, *Theory of Simple Liquids* (Academic, London, 1986).
[45] W. H. Press, B. P. Flannery, S. A. Teukolsky, and W. T. Vetterling, *Numerical Recipes* (Cambridge University Press, Cambridge, 1986), Chap. 3.
[46] M. P. Taylor, J. L. Mar, and J. E. G. Lipson, J. Chem. Phys. **106**, 5181 (1997).
[47] D. Frenkel and B. Smit, *Understanding Molecular Simulation* (Academic, London, 2002).
[48] G. Orkoulas and A. Z. Panagiotopoulos, J. Chem. Phys. **110**, 1581 (1999).
[49] Y. Mao, M. E. Cates, and H. N. W. Lekkerkerker, Physica A **222**, 10 (1995).